

ELECTRONIC SUPPLEMENTARY INFORMATION

**Pro-apoptotic and pro-differentiation induction by
8-quinolinecarboxaldehyde selenosemicarbazone and its Co(III) complex in
human cancer cell lines**

Nenad R. Filipović,^a Snežana Bjelogrić,^b Gustavo Portalone,^c Sveva Pelliccia,^d
Romano Silvestri,^d Olivera Klisurić,^e Milan Senćanski,^f Dalibor Stanković,^g
Tamara R. Todorović,^{h,*} Christian D. Muller^{i,*}

^a*Faculty of Agriculture, University of Belgrade, Nemanjina 6, Belgrade, Serbia.*

^b*National Cancer Research Center of Serbia, Pasterova 14, Belgrade, Serbia.*

^c*Dipartimento di Chimica, Sapienza Università di Roma, Piazzale Aldo Moro 5, I-00185 Roma, Italy.*

^d*Dipartimento di Chimica e Tecnologie del Farmaco, Sapienza Università di Roma, Piazzale Aldo Moro 5, I-00185 Roma, Italy.*

^e*Department of Physics, Faculty of Sciences, University of Novi Sad, Trg Dositeja Obradovića 4, Novi Sad, Serbia.*

^f*Center for Multidisciplinary Research, Institute of Nuclear Sciences "Vinča", University of Belgrade, Belgrade, Serbia*

^g*Innovation Center of the Faculty of Chemistry, University of Belgrade, Studentski trg 12-16, Belgrade, Serbia.*

^h*Faculty of Chemistry, University of Belgrade, Studentski trg 12-16, Belgrade, Serbia; E-mail: tamarat@chem.bg.ac.rs*

ⁱ*Institut Pluridisciplinaire Hubert Curien, UMR 7178 CNRS Université de Strasbourg, 67401 Illkirch, France; E-mail: cdmuller@unistra.fr*

Corresponding authors:

Tamara R. Todorović, E-mail: tamarat@chem.bg.ac.rs

Christian D. Muller, E-mail: cdmuller@unistra.fr

Supplementary Information:

Figure S1. ¹ H and ¹³ C NMR spectra of complex 1	2
Figure S2. 2D ROESY spectrum of complex 1	3
Figure S3. The electronic absorption spectra of the ligand and complex 1	4
Figure S4. Cyclic voltammograms of the ligand and 1	4
Table S1. Crystal data and structure refinement for the ligand H8qasesc and complex 1	5
Table S2. Selected geometrical parameters for H8qasesc and 1	6
Table S3. Selected dihedral angles (°) for H8qasesc and 1	7
Figure S5. The crystal packing of H8qasesc	8
Figure S6. Crystal packing in the crystal structure of complex 1	9
Table S4. Hydrogen bond and π - π stacking interaction parameters in the crystal structure of complex 1	10
Figure S7. ED ₅₀ values for CDDP and H8qasesc on THP-1 cell line	11
Figure S8. Activity of 1 on THP-1 cell line	12
Figure S9. Activity of CDDP on THP-1 cell line	13
Figure S10. Activity of caspase-8 and -9	14
Figure S11. The ligand H8qasesc and complex binding sites of HSA.....	15
Table S5. Quantified interactions of 1 in binding site of HSA	16
EXPERIMENTAL PART	17
Materials and methods	17
Synthesis of the ligand H8qasesc	18
Synthesis of the complex [Co(8qasesc) ₂]ClO ₄ ×DMSO (1)	18
Structure determination and refinement	19
Free radical-scavenging activity	19
Cell cultures and conditions	20
Determination of pro-apoptotic activity	20
Calculation of ED50 concentrations	21
Inhibition of caspase activity	21
Evaluation of caspase-8 and -9 activities	22
Investigation of pro-differentiation activity	22
DNA plasmid interactions	23
Molecular docking studies	24
REFERENCES	24

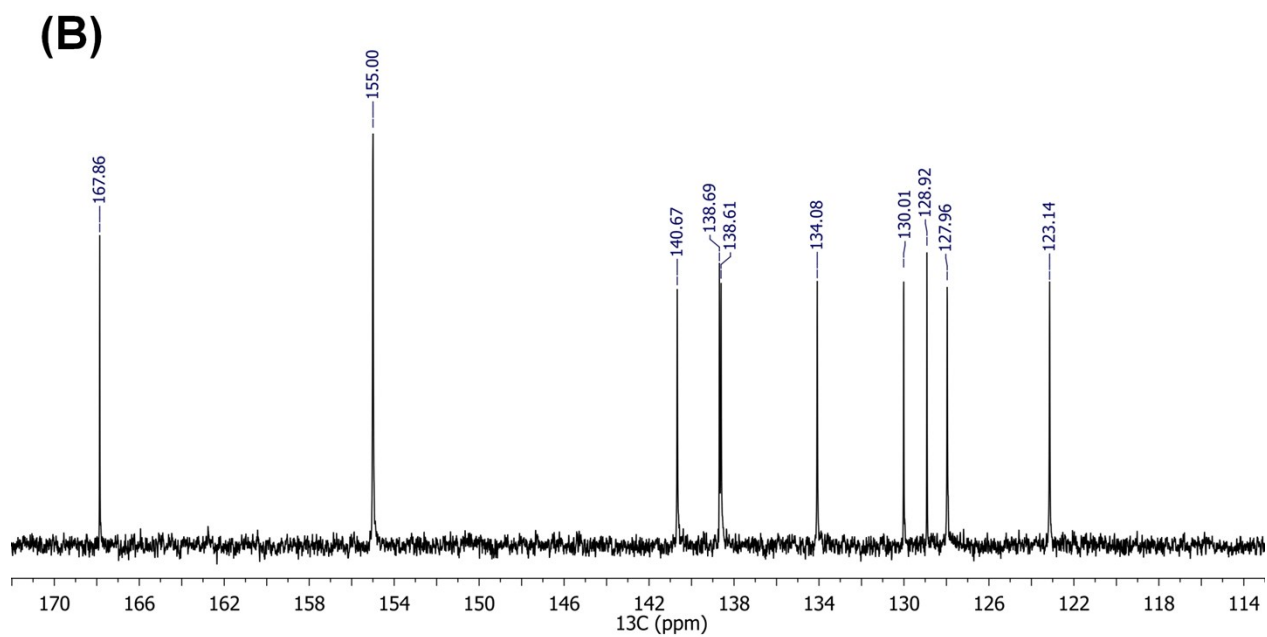
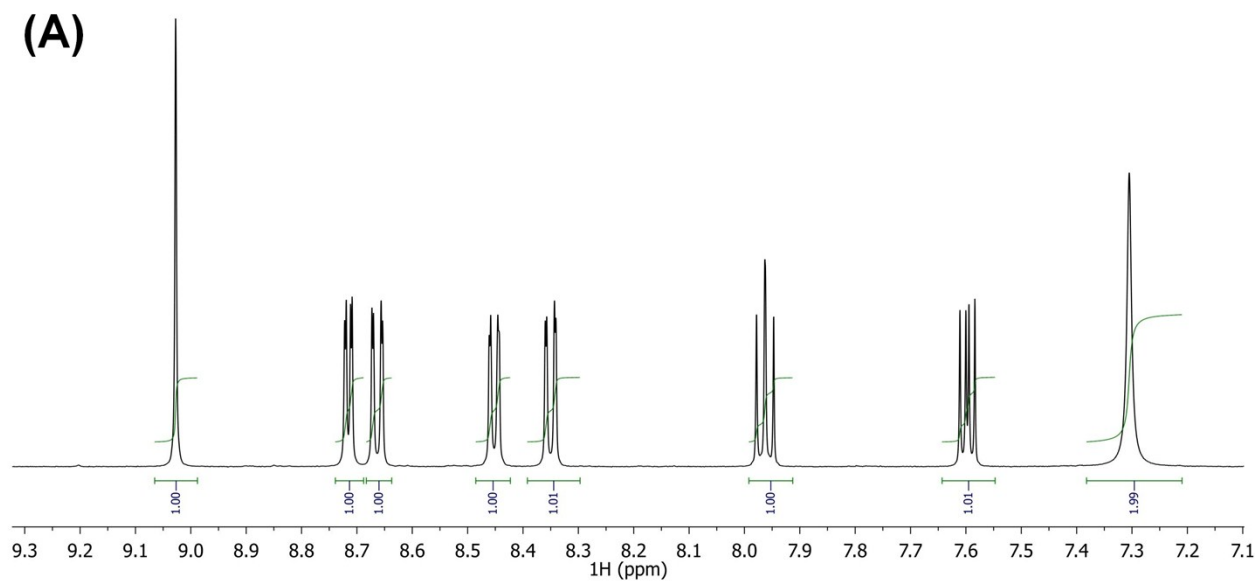


Figure S1. ^1H NMR (A) and ^{13}C NMR (B) spectra of complex **1**.

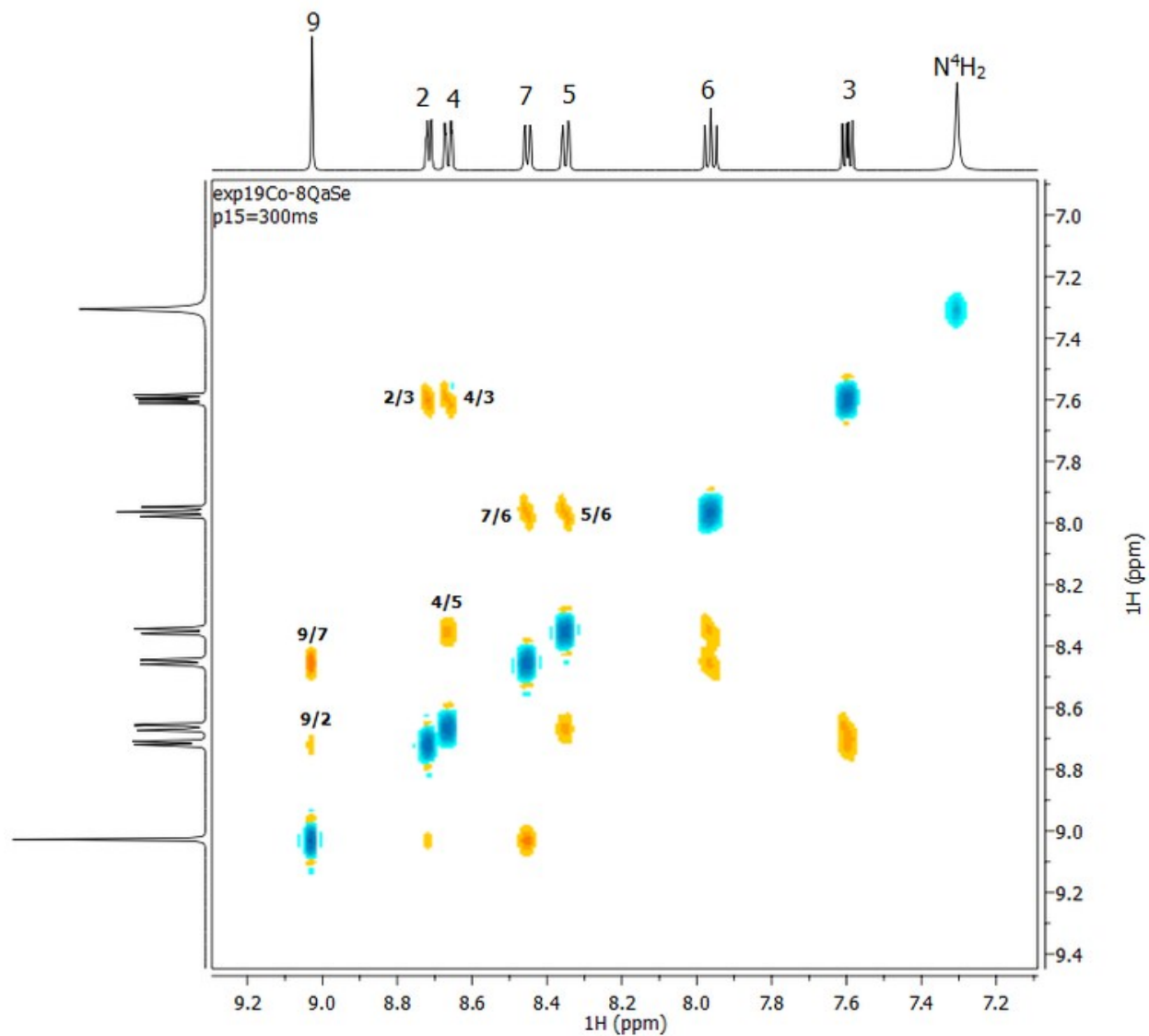


Figure S2. ROESY spectrum of the complex **1**.

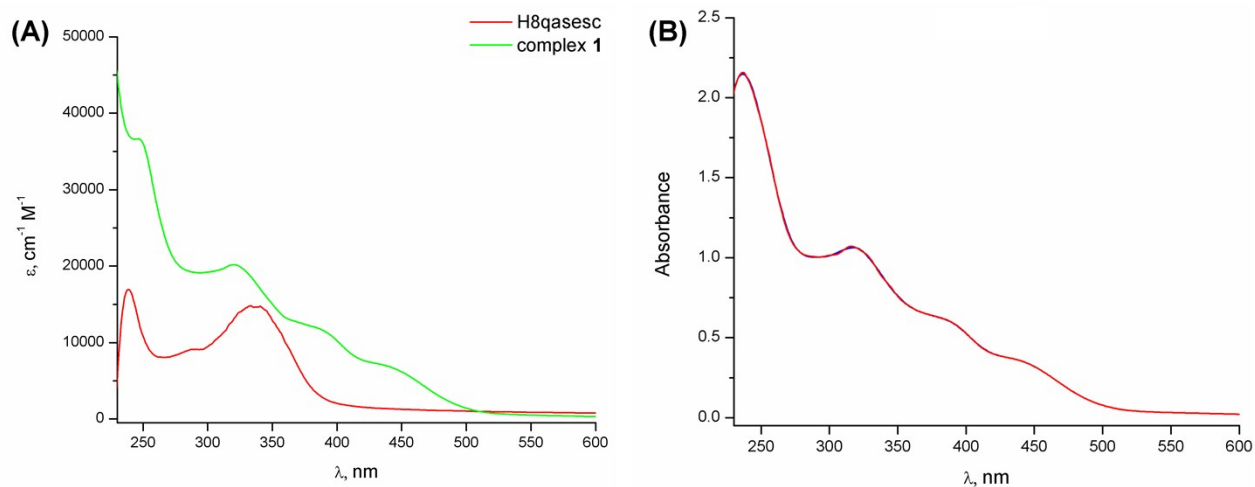


Figure S3. (A) The electronic absorption spectra of the ligand H8qasesc and complex **1** ($c = 5 \times 10^{-5}$ M) in methanol. (B) UV-Vis spectroscopy data of **1** in DMSO/H₂O 1 : 100 (v/v). First measurement (red), after 24 h (blue).

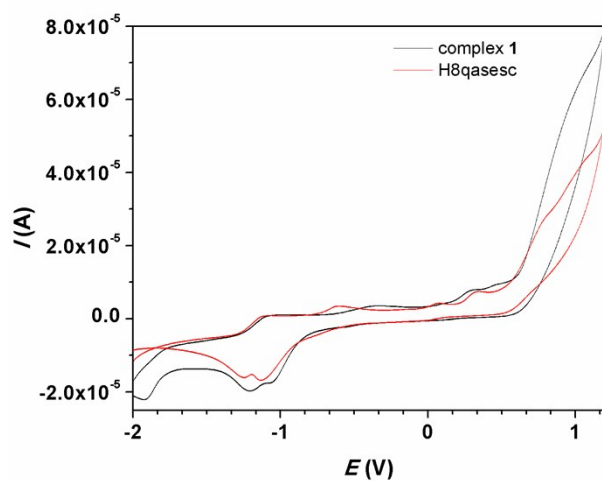


Figure S4. Cyclic voltammograms of H8qasesc (red) and **1** (black) in anhydrous DMSO containing 0.10 M [*n*-Bu₄N][PF₆] at scan rate of 100 mVs⁻¹ using a glassy carbon electrode.

Table S1. Crystal data and structure refinement for the ligand H8qasesc and complex **1**

	H8qasesc	1
Crystal data		
Empirical formula	C ₁₁ H ₁₀ N ₄ Se	C ₂₂ H ₁₈ CoN ₈ Se ₂ ·ClO ₄ · C ₂ H ₆ SO
Formula weight	277.19	788.82
Crystal system	Monoclinic	Triclinic
space group	<i>P</i> 2 ₁ / <i>c</i>	<i>P</i> -1
<i>a</i> , <i>b</i> , <i>c</i> (Å)	8.8291(8), 12.9308(8), 10.1657(7)	10.3102 (6), 10.7772 (6), 14.5496 (8)
α , β , γ (°)	90, 97.384(8), 90	80.932 (5), 89.859 (5), 65.526 (5)
<i>V</i> (Å ³)	1150.97 (15)	1449.47 (15)
<i>Z</i>	4	2
μ (mm ⁻¹)	3.24	3.32
Crystal size (mm)	0.33 × 0.25 × 0.11	0.09 × 0.08 × 0.08
Data collection		
<i>T</i> _{min} , <i>T</i> _{max}	0.719, 1.000	0.935, 1.000
No. of measured, independent and observed [<i>I</i> > 2σ(<i>I</i>) reflections	4093 2025 1668	21127 6302 5185
<i>R</i> _{int}	0.023	0.040
(sin θ/λ) _{max} (Å ⁻¹)	0.594	0.639
Refinement		
<i>R</i> [<i>F</i> ² > 2σ(<i>F</i> ²)]	0.031	0.038
<i>wR</i> (<i>F</i> ²)	0.075	0.094
<i>S</i>	1.02	1.02
No. of reflections	2025	6302
No. of parameters	161	389
Δ _{max} , Δ _{min} (e Å ⁻³)	0.51, -0.36	0.65, -0.52

Table S2. Selected geometrical parameters for H8qasesc and **1**.

H8qasesc		1	
Bond	Distance (Å)	Bond	Distance (Å)
Se1–C12	1.847(3)	Co1–N2	1.924(3)
N2–C11	1.271(3)	Co1–N2a	1.928(3)
N2–N3	1.372(3)	Co1–N1a	2.025(3)
N3–C12	1.334(4)	Co1–N1	2.036(3)
N4–C12	1.315(4)	Co1–Se2	2.3267(5)
N1–C2	1.311(4)	Co1–Se1	2.3345(6)
N1–C6	1.367(3)	Se1–C12	1.879(3)
C6–C5	1.411(4)	Se2–C12a	1.882(3)
C6–C10	1.422(4)	N2–C11	1.294(4)
C2–C3	1.453(4)	N2–N3	1.397(3)
C11–C10	1.377(4)	N3–C12	1.313(4)
		N4–C12	1.334(4)
		N2a–C11a	1.295(4)
		N2a–N3a	1.399(4)
		N3a–C12a	1.309(4)
		N4a–C12a	1.342(4)
Angle	(°)	Angle	(°)
C11–N2–N3	116.2(2)	N2a–Co1–N2	168.08(11)
C12–N3–N2	119.9(2)	N2a–Co1–N1a	95.77(11)
C2–N1–C6	117.1(3)	N2–Co1–N1a	93.44(11)
N4–C12–N3	118.4(3)	N2a–Co1–N1	93.14(11)
N4–C12–Se1	122.3(2)	N2–Co1–N1	94.82(11)
N3–C12–Se1	119.3(2)	N1a–Co1–N1	87.48(11)
N1–C6–C5	121.9(3)	N2a–Co1–Se1	85.30(8)
N1–C6–C10	118.7(2)	N2–Co1–Se2	84.04(8)
C5–C6–C10	119.3(2)	N1a–Co1–Se2	177.20(8)
N2–C11–C10	120.8(3)	N1–Co1–Se2	91.52(8)
C9–C10–C6	118.7(2)	N2a–Co1–Se2	86.89(8)
		N2–Co1–Se1	87.19(8)
		N1a–Co1–Se1	89.69(8)
		N1–Co1–Se1	176.61(8)
		Se2–Co1–Se1	91.39(2)

Table S3. Selected dihedral angles (°) for H8qasesc.

C11–N2–N3–C12	–177.6(2)
N2–N3–C12–N4	–0.1(4)
N2–N3–C12–Se1	178.20(19)
C2–N1–C6–C5	1.6(4)
C2–N1–C6–C10	–177.6(2)
N3–N2–C11–C10	179.0(2)
N1–C6–C10–C9	–178.6(3)
C6–N1–C2–C3	–0.4(5)
N4–C8–C7–C6	177.6(3)
C10–C6–C5–C7	–3.1(4)
N1–C6–C10–C11	0.6(4)
C5–C6–C10–C11	–178.7(2)
N2–C11–C10–C9	–4.3(4)
N2–C11–C10–C6	176.5(2)
C6–C10–C9–C8	0.1(4)
C11–C10–C9–C8	–179.1(3)
N1–C6–C5–C4	–1.7(4)
C10–C6–C5–C4	177.6(2)
C7–C5–C4–C3	–178.9(3)
N1–C2–C3–C4	–0.8(5)

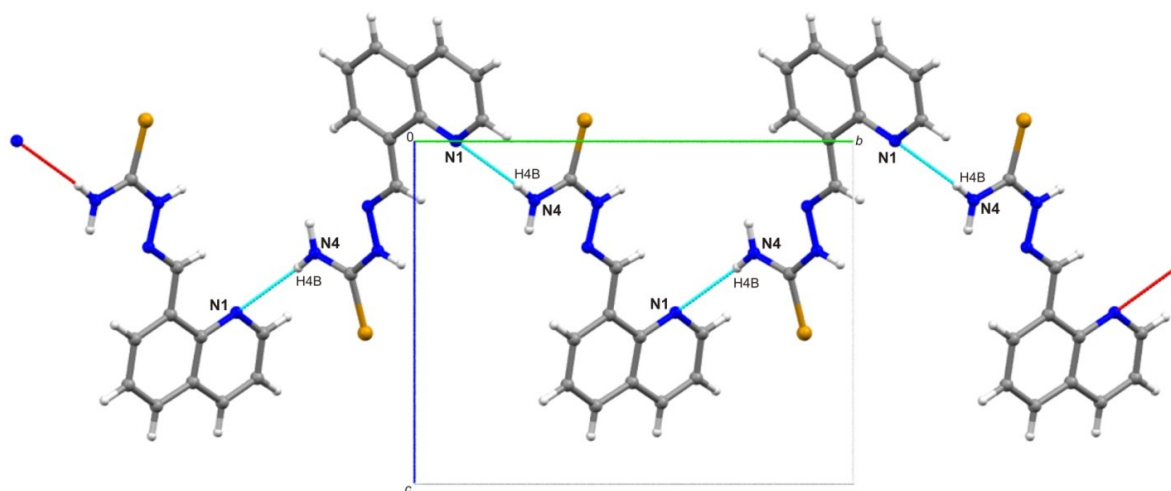


Figure S5. The crystal packing of H8qasesc viewed along a -axis. Hydrogen bonds are shown as light blue dashed line. The molecules of H8qasesc in the crystal structure are connected to a head-to-tail one dimensional polymer by $N4-H4B \cdots N1 [1-x, 1/2+y, 3/2-z]$ hydrogen bond ($N4 \cdots N1 = 3.191(4) \text{ \AA}$; $N4-H4B = 0.80(3) \text{ \AA}$; $H4B \cdots N1 = 2.41(3) \text{ \AA}$; $\angle N4-H4B-N1 = 166^\circ$).

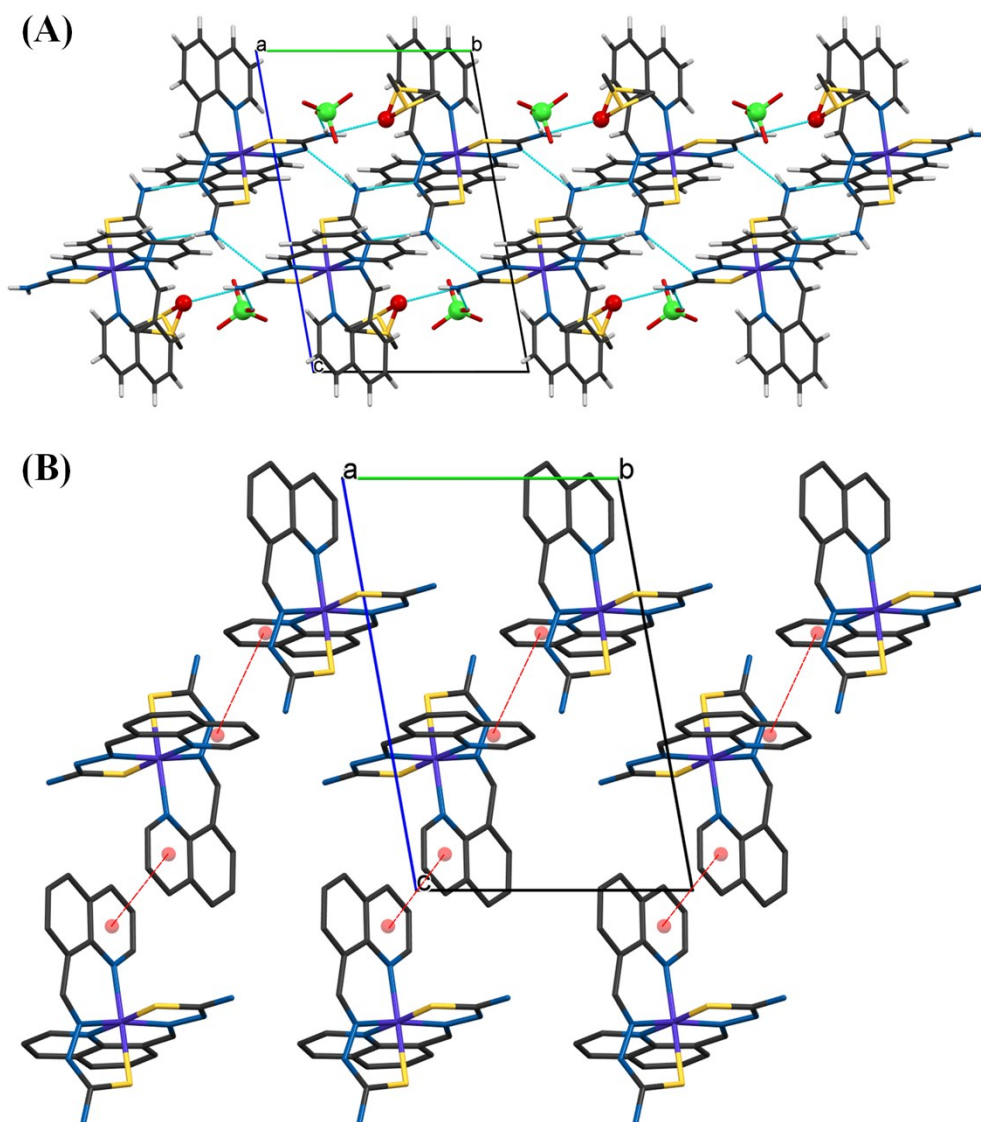


Figure S6. Crystal packing in the crystal structure of complex **1** viewed along the *a*-axis. Color code: chlorine – green, oxygen – red, cobalt - purple, nitrogen – blue, selenium – yellow, carbon – grey, hydrogen – white. (A) Infinite 1-D chains, formed by hydrogen bonding, parallel to the *b*-axis. Perchlorate anions and solvent DMSO molecules also participate in the hydrogen bonding. (B) π - π stacking interactions of quinoline fragments (red dashed lines); perchlorate anions, DMSO solvent molecules and hydrogen atoms are omitted for clarity. The stacking interactions between neighboring pyridine fragments expand 1-D chains formed by hydrogen bonding into 2-D supramolecular layers parallel to (001). Finally, these 2-D layers are further interlinked into a 3-D framework by additional stacking interactions.

Table S4. Hydrogen bond and π - π stacking interaction parameters in the crystal structure of complex **1**.

H-bond parameters					
D-H \cdots A	D-H (Å)	H \cdots A (Å)	D \cdots A (Å)	D-H \cdots A (°)	symmetry operation on A
N4A-H4A1 \cdots O1	0.86	2.09	2.908(4)	160	
N4A-H4A2 \cdots O4	0.86	2.13	2.978(9)	168	
N4-H41 \cdots N3	0.86	2.13	2.974(4)	169	$2-x, 1-y, 1-z$
N4-H42 \cdots N3A	0.86	2.38	3.189(4)	157	$2-x, -y, 1-z$
π - π interaction parameters					
Cg(I),Cg(J) ^a Cg-Cg ^b (Å)	α^c (°)	β^d (°)	γ^e (°)	slippage ^f (Å)	symmetry operation on J
complex 3					
Cg1, Cg1 4.017(2)	0.01(1)	29.6	29.6	1.987	$2-x, -y, 2-z$
Cg2, Cg2 4.011(2)	0.03(2)	31.5	31.5	2.097	$1-x, 1-y, 1-z$

^a Planes of the rings I/J: ring (1) = N(1),C(2),C(3),C(4),C(5),C(10); ring (2) = N(1A),C(2A),C(3A),C(4A),C(5A),C(10A)

^b Cg-Cg = distance between ring centroids (Å).

^c α = dihedral angle between planes I and J (°).

^d β = angle between Cg(I),Cg(J) vector and normal to plane I (°).

^e γ = angle between Cg(I), Cg(J) vector and normal to plane J (°).

^f Slippage = distance between Cg(I) and perpendicular projection of Cg(J) on ring I (Å).

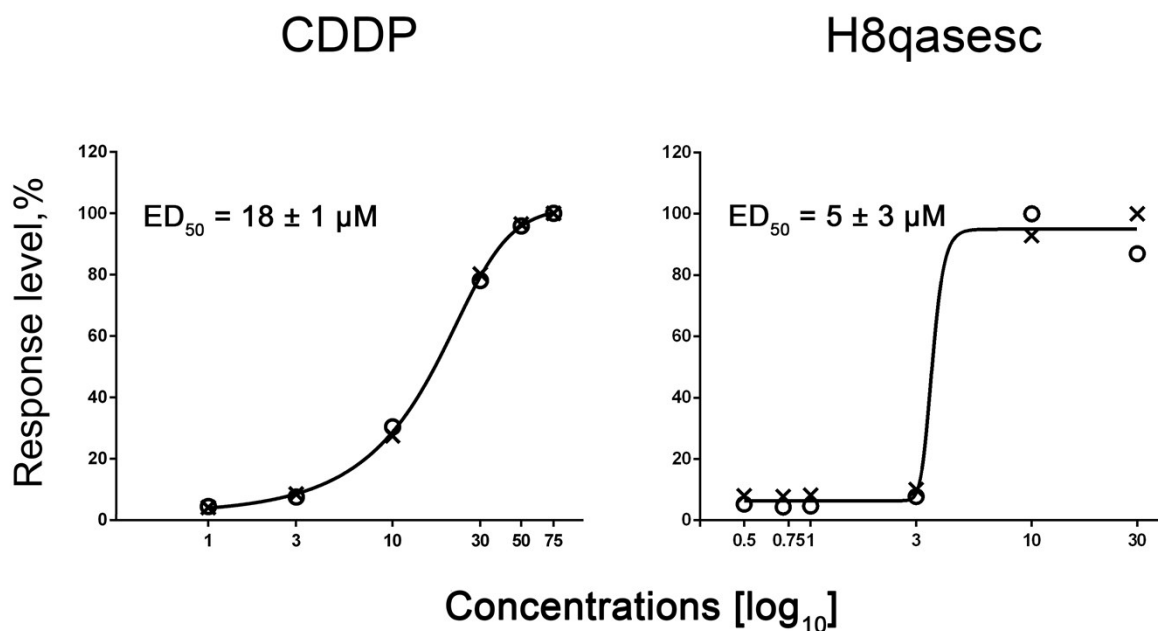


Figure S7. ED₅₀ values for CDDP and H8qasesc on THP-1 cell line. THP-1 cells were treated with CDDP and H8qasesc applied in a range of six concentrations for 24 h, and afterwards stained with Annexin-V and PI. Percentages of all Annexin-V labeled cells for each concentration of investigated compounds were calculated as a proportion of the maximal apoptotic response normalized as 100%. Such scaled apoptotic outcomes were plotted against concentrations and ED₅₀ concentration was calculated using asymmetric sigmoidal curve five-parameter logistic equation (GraphPad Prism 6 software).

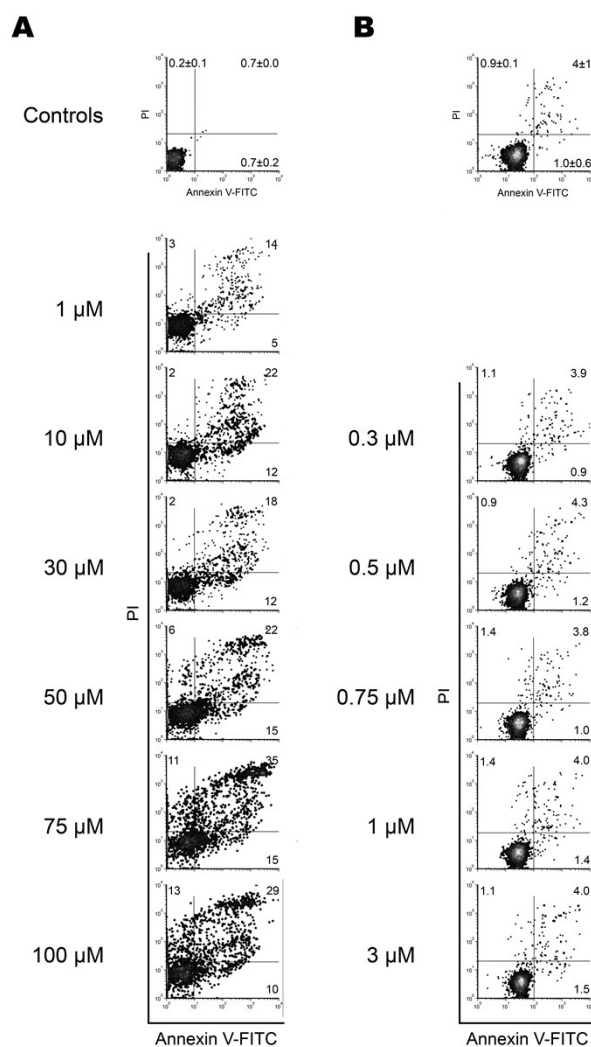


Figure S8. Activity of **1** on THP-1 cell line. Annexin-V and propidium iodide (PI) double staining THP-1 cells after 24 h treatment with **1** applied in a concentration range 1-100 μM (**A**) and in a low concentration range 0.3-3 μM (**B**). In Annexin-V/PI plots cells are discriminated as viable (non-stained cells, lower left quadrant), cells in early phases of apoptosis (Annexin-V single stained cells, lower right quadrant), cells in late phases of apoptosis (double-stained cells, upper right quadrant), and cells in necrosis (PI single stained cells, upper left quadrant). Results are represented as a single replicate considering the second experiment was not performed due to the high percentage of necrotic cells induced by the treatment with **1** on this cell line.

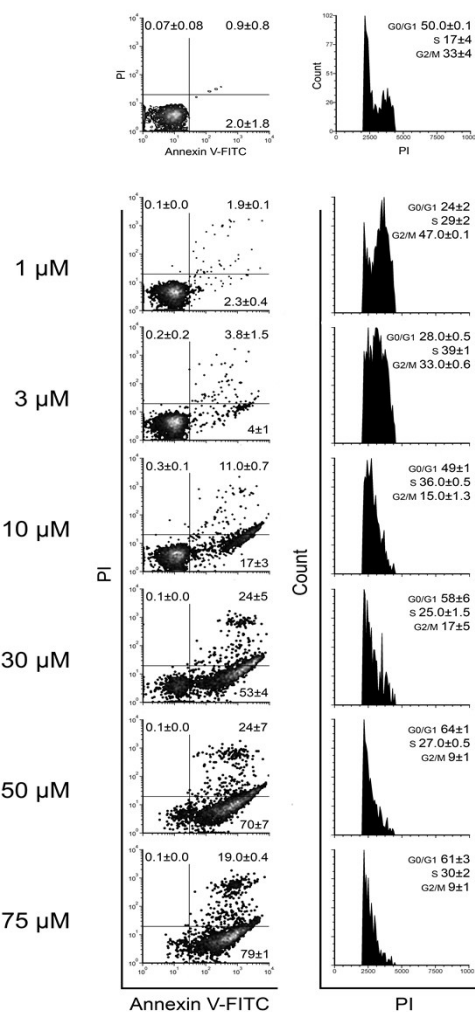


Figure S9. Activity of CDDP on THP-1 cell line. Annexin-V and propidium iodide (PI) double staining (left panels) and PI single staining (right panels) of THP-1 cells after 24 h treatment with CDDP applied in a range of six concentrations. In Annexin-V/PI plots cells are discriminated as viable (non-stained cells, lower left quadrant), cells in early phases of apoptosis (Annexin-V single stained cells, lower right quadrant), cells in late phases of apoptosis (double-stained cells, upper right quadrant), and cells in necrosis (PI single stained cells, upper left quadrant). The same cells evaluated with Annexin-V/PI were fixed in ethanol right after analysis, left overnight and afterwards assayed for distribution within phases of mitotic division with PI single staining method. Frequency of cells found in G0/G1, S and G2/M phases was determined according to non-treated control population. All results are expressed as the mean % \pm SD of two replicates from independent experiments.

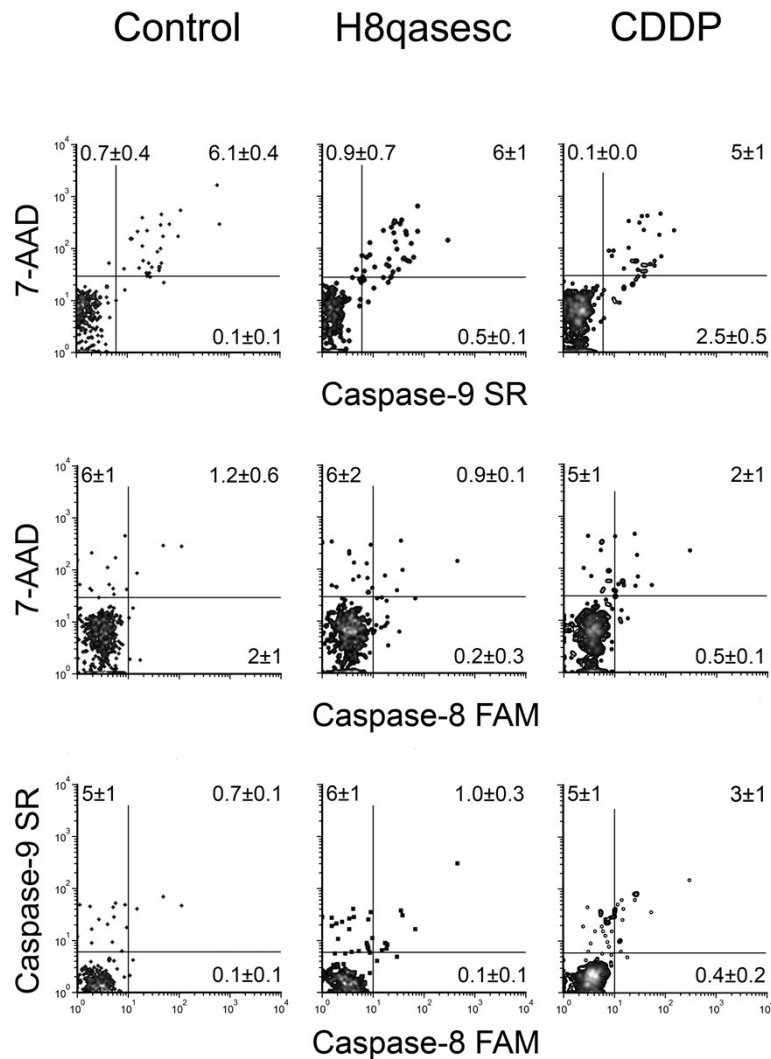


Figure S10. Activity of caspase-8 and -9 in non-treated and treated THP-1 cells. Caspase-8 and -9 activities were determined after 6 h incubation with H8qasesc and CDDP applied at their ED_{50} concentrations. In the plots cells are discriminated as live (not stained with either caspase nor 7-AAD), mid stage apoptotic cells (cells stained with either caspase-8 or -9, but negative to 7-AAD), late stage apoptotic cells (cells stained with either of caspase-8 or -9 and with 7-AAD), and necrotic cells (cells not stained with either caspase-8 nor -9, but positive for 7-AAD). Results are expressed as the mean % \pm SD of two replicates from independent experiments.

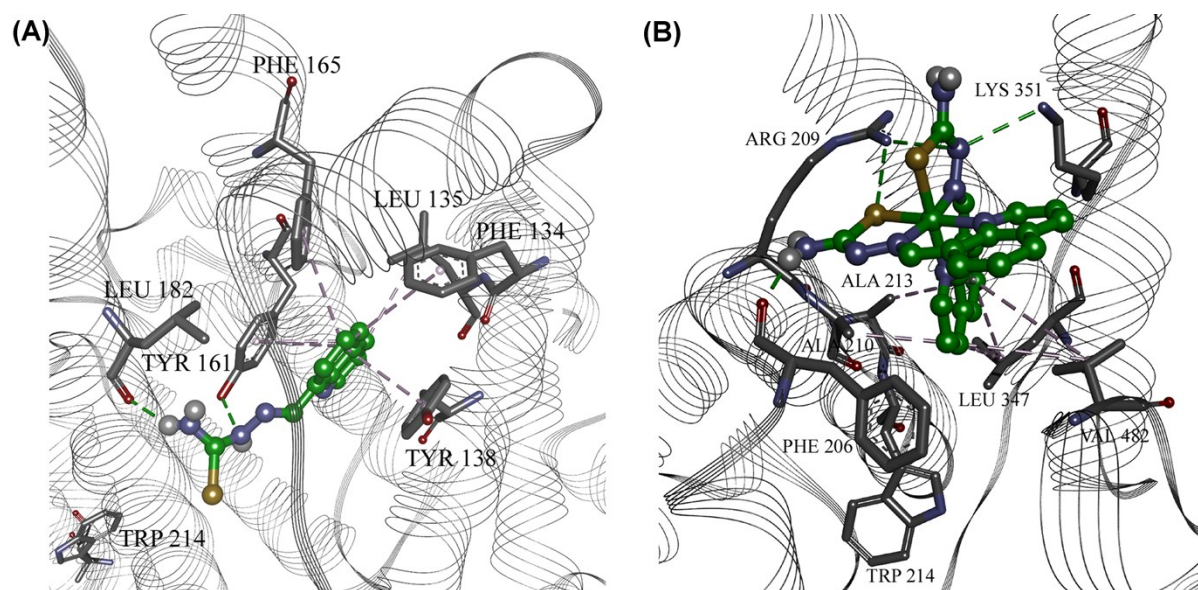


Figure S11. (A) The ligand H8qasesc in heme binding site of HSA (PDB ID 1BJ5), with marked amino acid residues and interactions. The interactions in the binding pocket include hydrophobic/aromatic with Leu 182, Tyr 161, Phe 165, Leu 135, Phe 134 and Tyr 138. Hydrophilic interactions include hydrogen bonds with Tyr 161 and Leu 182 (*via* carbonyl oxygen). (B) The complex **1** in binding site of HSA, with marked amino acid residues and interactions. Selected conformation with the lowest binding energy ($-35.58 \text{ kJ mol}^{-1}$). The main electrostatic interaction is formed with Arg 209 and Lys 351, with partially negatively charged (and acidic) nitrogen atoms. Although the complex cation is +1 charged, the electrostatic interaction with Glu 354 is not formed. The rest of interactions are hydrophobic type CH- π and aromatic, including interaction of residues Leu 347, Ala 210, Ala 213 and Val 482. Green: hydrogen bonds; Grey: hydrophobic/aromatic interactions.

Table S5. Quantified interactions of **1** with aminoacid residues in binding site of HSA.

Residue (atom)	Interaction type	Distance / Å
Phe 206 (carbonyl O)	Hydrogen bond	1.985
Ala 210	Hydrophobic	3.847
Ala 213	Hydrophobic	4.376
Leu 347	Hydrophobic	4.023
Leu 347	Hydrophobic	5.188
Lys 351	Hydrogen bond	3.284
Val 482	Hydrophobic	5.394
Val 482	Hydrophobic	4.729
Arg 209 (NH1) - N _{sp2}	Hydrogen bond	3.372
Arg 209 (NH1) - Se	Hydrogen bond	3.462

EXPERIMENTAL PART

Materials and methods

All the employed reagents and solvents were of analytical grade and used without further purification. 8-Quinolinecarboxaldehyde (8qa) was obtained from MAYBRIDGE (England), while cobalt(II) perchlorate hexahydrate was obtained from Aldrich (Sigma-Aldrich Chemie GmbH, Steinheim, Germany).

Elemental analyses (C, H, N) were performed by the standard micromethods using the ELEMENTARVario ELIII C.H.N.S=O analyzer. Infrared (IR) spectra were recorded on a Thermo Scientific Nicolet 6700 FT-IR spectrophotometer by the attenuated total reflection (ATR) technique in the region 4000–400 cm^{-1} . Abbreviations used for IR spectra: vs, very strong; s, strong; m, medium; w, weak. UV-Visible (UV-Vis) spectra were recorded on a GBC Scientific Eq. PTY LTD Cintra 6 UV-Vis spectrophotometer (900–220 nm), using samples dissolved in methanol. Molar conductivity measurements were performed at ambient temperature on the Crison Multimeter MM41. The 1D (^1H and ^{13}C) and 2D NMR spectra were performed on Bruker Avance 500 equipped with broad-band direct probe. All spectra were measured at 298 K. Chemical shifts are given on δ scale relative to tetramethylsilane (TMS) as internal standard for ^1H and ^{13}C . Abbreviations used for NMR spectra: s, singlet; d, doublet; dd, double doublet; t, triplet; q, quartet; br. broad. Atom numbering used in NMR is shown in Scheme 1. The magnetic measurement at room temperature was performed by Evans' method using a MSB-MK1 balance (Sherwood Scientific Ltd.) with $\text{Hg}[\text{Co}(\text{SCN})_4]$ as a calibrant. Cyclic voltammetric measurements were performed using an electrochemical system CH Instruments (USA). The cell (10 mL) consisted of three-electrode system, glassy carbon electrode (inner diameter of 3 mm; CHI 104) an Ag/AgCl (saturated KCl) reference electrode and Pt counter electrode. The potential was swept over the range from -2.0 to $+1.2$ V (*vs.* Ag/AgCl) at scan rate of 100 mVs^{-1} . Measurements were performed at room temperature with deaeration of solutions by passing a stream of nitrogen through the solution for 5 min prior to the measurement and then maintaining a blanket atmosphere of nitrogen over the solution during the measurement. The potentials were measured in $0.10 \text{ M } [n\text{-Bu}_4\text{N}]\text{PF}_6 / \text{DMSO}$, and are quoted relative to Ag/AgCl reference electrode.

Synthesis of the ligand H8qasesc

The ligand H8qasesc was synthesized according to the reported procedure [S1]. Its structure was confirmed by elemental analysis, IR and NMR spectroscopy. Single crystals of H8qasesc suitable for X-ray analysis were obtained by slow diffusion of ethanol into its DMSO solution of the ligand.

H8qasesc: Anal. Calcd. for $C_{11}H_{10}N_4Se$ (MW = 277.18): C, 47.66; H, 3.64; N, 20.21. Found: C, 47.81; H, 3.82; N, 20.12 %. IR (ATR, cm^{-1}): 3363, 3268, 3124, 3030, 2976, 1603, 1572, 1535, 1499, 1472, 1392, 1336, 1263, 1104, 1032, 946, 830, 785, 636, 594. 1H NMR (500 MHz, DMSO- d_6) δ (ppm): 7.60 (dd, 1H, H-C3, $^3J_{3,4} = 8.3$ Hz, $^3J_{3,2} = 4.2$ Hz), 7.65 (t, 1H, H-C6, $^3J_{6,7} = ^3J_{6,5} = 7.7$ Hz), 8.06 (dd, 1H, H-C5, $^3J_{5,6} = 7.7$ Hz, $^4J_{5,7} = 1.2$ Hz), 8.42 (dd, 1H, H-C4, $^3J_{4,3} = 8.3$ Hz, $^4J_{4,2} = 1.7$ Hz), 8.63 (s, 1H, H^a-N4), 8.66 (dd, 1H, H-C7, $^3J_{7,6} = 7.7$ Hz, $^4J_{7,5} = 1.2$ Hz), 8.70 (s, 1H, H^b-N4), 8.97 (dd, H-C2, $^3J_{2,3} = 4.1$ Hz, $^4J_{2,4} = 1.7$ Hz), 9.44 (s, 1H, H-C9), 11.96 (s, 1H, H-N3). ^{13}C NMR (126 MHz, DMSO- d_6) δ (ppm): 121.82 (C3), 126.34 (C6), 126.40 (C7), 127.96 (C4a), 130.05 (C5), 131.00 (C8), 136.59 (C4), 140.61 (C9), 145.43 (C8a), 150.43 (C2), 173.89 (C10).

Synthesis of the complex [Co(8qasesc)₂](ClO₄)₂·DMSO (1)

Into the suspension of 8-quinolinecarboxaldehyde (0.10 g, 0.63 mmol) and selenosemicarbazide (0.09 g, 0.64 mmol) in ethanol (10 mL), solid $Co(ClO_4)_2 \cdot 6H_2O$ (0.12 g, 0.32 mmol) was added. The reaction mixture was stirred under the reflux for 2 h. Brown microcrystalline product was filtered off and washed with cold ethanol and diethyl ether. Dark brown single crystals of **1** were obtained by slow diffusion of ethanol into the DMSO solution of the complex. Yield: 0.16 g (52.6%). Anal. Calcd. for $C_{24}H_{24}N_8O_5Se_2SClCo$ (MW = 788.86): C, 36.54; H, 3.07; N, 14.20; S, 4.06. Found: C, 36.72; H, 3.12; N, 14.12; S, 4.12 %. IR (ATR, cm^{-1}): 3405, 3293, 3112, 1643, 1621, 1595, 1496, 1385, 1323, 1260, 1184, 1093, 913, 830, 779, 708, 655, 623, 584, 553, 525, 460, 418. 1H NMR (500 MHz, DMSO- d_6) δ (ppm): 2.54 (s, 3H, DMSO), 7.30 (s, 2H, H-N4), 7.60 (dd, 1H, H-C3, $^3J_{3,4} = 8.1$ Hz, $^3J_{3,2} = 5.3$ Hz), 7.96 (t, 1H, H-C6, $^3J_{6,5} = ^3J_{6,7} = 7.6$ Hz), 8.35 (dd, 1H, H-C5, $^3J_{5,6} = 7.6$ Hz, $^4J_{5,7} = 1.3$ Hz), 8.45 (dd, 1H, H-C7, $^3J_{7,6} = 7.6$ Hz, $^4J_{7,5} = 1.1$ Hz), 8.66 (dd, 1H, H-C4, $^3J_{4,3} = 8.1$ Hz, $^4J_{4,2} = 1.4$ Hz), 8.72 (dd, 1H, H-C2, $^3J_{2,3} = 5.3$ Hz, $^4J_{2,4} = 1.4$ Hz), 9.03 (s, 1H, H-C9). ^{13}C NMR (126 MHz, DMSO- d_6) δ (ppm): 40.42 (DMSO), 123.14 (C3), 127.96 (C6), 128.92 (C8), 130.01 (C4a), 134.08 (C5), 138.61 (C7),

138.69 (C8a), 140.67 (C4), 155.00 (C2 and C9), 167.86 (C10). M_M ($1 \cdot 10^{-3}$ M, DMSO): $32.1 \Omega^{-1} \text{ cm}^2 \text{ mol}^{-1}$. UV-Vis (MeOH), λ_{max} , nm (ϵ , $\text{M}^{-1} \text{ cm}^{-1}$): 246 (36603), 320 (20176), 386sh (11848), 438sh (6937). Magnetic measurements showed that obtained complex is diamagnetic.

Structure determination and refinement

A suitable single crystal of H8qasesc ligand and its Co(III) complex were mounted on a glass fiber and crystallographic data were collected using an Oxford Diffraction Gemini S diffractometer with a CCD area detector ($\lambda_{\text{MoK}\alpha} = 0.710689 \text{ \AA}$, monochromator: graphite). The CrysAlisPro and CrysAlis RED software packages [S2] were used for data collection and data integration. Collected data were corrected for absorption effects by using an Multi-scan absorption correction [S3]. Structure solution and refinement were carried out with the programs SHELXS and SHELXL-2014/7, respectively [S4]. All non-hydrogen atoms were refined anisotropically until convergence was reached. The hydrogen atoms were located in a difference Fourier map and refined isotropically, with the exception of those H atoms linked to the C atoms and those H atoms linked to the N atoms which were placed in calculated positions (C–H = 0.97 \AA , N–H = 0.86 \AA , U_{iso} values equal to $1.2 U_{\text{eq}}$ C, N) and allowed to ride on their carrier atoms. In **1**, the solvent molecule (DMSO) is disordered over two positions and therefore the hydrogen atoms of the crystalline solvent were not positioned and refined. CCDC 1471189 and CCDC 1401687 contain the supplementary crystallographic data for the ligand H8qasesc and complex **1**, respectively. This data can be obtained free of charge via <https://summary.ccdc.cam.ac.uk/structure-summary-form>, or from the Cambridge Crystallographic Data Centre, 12 Union Road, Cambridge CB2 IEZ, UK; fax: (+044)1223-336-033; or e-mail: deposit@ccdc.cam.ac.uk.

Free radical-scavenging activity

The proton donating ability was assayed using the protocol for determination of radical scavenging activity [S5]. Compounds were dissolved in pure DMSO and were diluted into ten different concentrations. Commercially-available free radical 1,1-diphenyl-2-picryl-hydrazyl (DPPH) was dissolved in methanol at concentration 6.58×10^{-5} M. Into a 96-well microplate,

140 μ L of DPPH solution was loaded and 10 μ L DMSO solution of the tested compounds was added, or pure DMSO (10 μ L) as the control. The microplate was incubated for 30 min at 25 °C in the dark and the absorbance was measured at 517 nm using Thermo Scientific Appliskan. All the measurements were carried out in triplicate. Free radical scavenging activity was calculated using the following equation:

$$\text{Scavenging activity (\%)} = \frac{A_{\text{control}} - A_{\text{sample}}}{A_{\text{control}}} \times 100$$

A_{sample} and A_{control} refer to the absorbances at 517 nm of DPPH in the sample and control solutions, respectively.

Cell cultures and conditions

Acute monocytic leukemia cell line (THP-1, ATCC® TIB-202) and pancreatic adenocarcinoma cell line (AsPC-1, ATCC® CRL-1682) were maintained in RPMI-1640 (Life Technologies, 11875-093) and DMEM high glucose (Sigma-Aldrich, D5796) cell culture media, respectively. Both media were supplemented with 10% (v/v) fetal bovine serum (FBS, Gibco, Cat. No. 16000-036) and 1% (v/v) penicillin-streptomycin (10 000 units/mL and 10 000 μ g/mL, Gibco, Cat. No. 15140-130). Cells were kept at 37 °C in atmosphere containing 5% (v/v) CO₂ during their exponential growth and during the course of experimental treatments. Investigated compounds were initially dissolved in DMSO to the stock concentration of 20 mM. Further dilutions to the experimental concentrations applied on the cells have been done with RPMI-1640 or DMEM media immediately before each experiment, thus the final concentration of DMSO on cells treated with the highest applied concentration was 0.5% (v/v).

Determination of pro-apoptotic activity

THP-1 and AsPC-1 cells were seeded in 96 flat bottom well plates (Corning® Costar®, Cat. No. CLS3596) in 0.1 mL, at a density of 10 000 per well. Since THP-1 cells grow in suspension, experimental treatments started within 2 h after cells seeding, while plates with seeded AsPC-1 cells were left overnight to settle. Investigated compounds were added in a range of six concentrations. As controls, we used non-treated cells, cells treated with 0.5% DMSO, and

cells treated by Celastrol (Enzo Life Sciences, Cat. No. ALX-350-332-M025) at 50 μ M concentration. After 24 h of incubation, THP-1 cells were centrifuged (RCF = 450g, 10 min), supernatants were discarded, and 0.1 mL of phosphate buffer saline (PBS) was added to each well. Plates were placed on plate shaker for 3 min, afterwards Annexin-V–FITC (ImmunoTools, Cat. No. 31490013) and propidium iodide (PI, Miltenyl Biotec, Cat. No. 130-093-233) were added in a volume of 3 μ L per well, respectively, and incubated for 15 min in the dark before cytometry analysis. Post incubation manipulation with AsPC-1 cells included trypsinization (200 μ L of trypsin per well, Sigma-Aldrich, Cat. No. T3924). Subsequent steps with addition of PBS, Annexin-V and PI were the same as for THP-1 cells. Plates were analyzed on Guava EasyCyte™ micro-capillary flow cytometer (EMD Millipore, Darmstadt, Germany) using InCyte® software package (EMD Millipore, Cat. No. 0500-4120). Cells were classified according to Annexin-V and PI labeling on viable (non-stained cells), pre-apoptotic cells (stained with Annexin-V only), cells in late phases of apoptosis (double stained cells), and necrotic cells (stained with PI only). After analysis, remaining cells were fixed in ethanol overnight at 4 °C, stained with FxCycle™ PI/RNase Staining solution (Molecular Probes, Cat. No. F10797), then analyzed as described previously [S6].

Calculation of ED₅₀ concentrations

Separately for THP-1 and AsPC-1 cells, percent of Annexin-V labeled cells for each investigated concentration of compounds were summarized and maximum apoptotic response was normalized to 100%. Percent of apoptosis read out for other concentrations were calculated as a proportion of the highest response. Such scaled apoptotic outcomes were plotted against concentrations and ED₅₀ concentration was calculated using asymmetric sigmoidal curve five-parameter logistic equation (GraphPad Prism 6 software). Obtained ED₅₀ concentrations values of both compounds were applied in further steps of this investigation.

Inhibition of caspase activity

Cells were treated with investigated compound at ED₅₀ concentration for 6 h with or without pan-caspase inhibitor *N*-benzyloxycarbonyl-Val-Ala-Asp(OMe) fluoromethyl ketone (Z-VAD-fmk, Promega, Cat. No. G7232). As controls, non-treated cells, cells treated with Z-VAD-

fmk only, and cells treated with ED₅₀ concentration only were used. After incubation period was ended, samples with treated cells were carried out for Annexin-V/PI staining as described above then monitored on Guava EasyCyte™ cytometer. The percent of apoptosis inhibited by Z-VAD-fmk co-treatment was computed by the formula:

$$\text{Inhibition, \%} = [1 - (\% \text{ of apoptosis in A} / \% \text{ of apoptosis in B})] \times 100,$$

where A is the sample treated with both ED₅₀ and Z-VAD-fmk, while B is the corresponding sample treated with ED₅₀ only.

Evaluation of caspase-8 and -9 activities

Cells treated with investigated compound at ED₅₀ concentration for 6 h afterwards activity of caspase-8 and -9 were assayed by means of Guava Caspase 9 SR and Caspase 8 FAM kit (EMD Millipore, Cat. No. 4500-0640), following manufacturer's instructions. In acquired data cells were discriminated according to expression of green fluorescence (caspase-8), yellow fluorescence (caspase-9), or red fluorescence (7-AAD) as the following: live cells (not stained with either caspase nor 7-AAD); mid-stage apoptotic cells (cells stained with either caspase-8 or -9, but negative to 7-AAD); late stage apoptotic cells (cells stained with either of caspase-8 or -9 and with 7-AAD); necrotic cells (cells not stained with either caspase-8 nor -9, but positive for 7-AAD).

Investigation of pro-differentiation activity

AsPC-1 cells were seeded in a volume 0.1 mL, at density 5000 per well of 96 well flat bottom plates. After 24 h, H8qasesc and **1** were added in a volume of 0.2 mL to the final concentrations of 1 and 10 μM per well. Wells with control cells were supplemented with medium up to the volume of 0.3 mL. All cells, treated and non-treated controls, were incubated for another 72 h, afterwards evaluation of changes in expression of cell surface markers of differentiation has been performed. In brief, when incubation was ended, supernatant was discarded after plate centrifugation for 10 min at RCF of 450g. A 0.1 mL of PBS was added to each well, plate was put on a plate shaker for 5 min, after anti-CD44-FITC (Miltenyl Biotec, Cat No 130-095-195) and anti-CD-133-PE (Miltenyl Biotec, Cat No 130-181-801) were added in a volume of 1 μM to each well. Non-treated controls were labeled with anti-CD44-FITC, anti-

CD133-PE, anti-IgG-FITC (Miltenyl Biotec, Cat No 130-093-192), or anti-IgG-PE (Miltenyl Biotec, Cat No 190-93-193). Plates incubated at 37 °C for 30 min, were additionally washed with PBS to remove excess of antibodies. The plate was then monitored on Guava EasyCyte™ micro-capillary flow cytometer for green and yellow fluorescence intensities. Results were analyzed using FlowJo version X software package.

DNA plasmid interactions

For DNA cleavage experiments the plasmid pUC19 (2686 bp, purchased from Sigma-Aldrich, USA) was prepared by its transformation in chemically competent cells *Escherichia coli* strain XL1 blue. Amplification of the clone was done according to the protocol for growing *E. coli* culture overnight in LB medium at 37 °C [S7] and purification was performed using Qiagen Plasmid plus Maxi kit. Finally, DNA was eluted in 10 mM Tris-HCl buffer and stored at -20 °C. The concentration of plasmid DNA (460 ng/μL) was determined by measuring the absorbance of the DNA-containing solution at 260 nm. One optical unit corresponds to 50 μg/mL of double stranded DNA.

The cleavage reaction of supercoiled pUC19 DNA due to different treatments was investigated by incubation of 460 ng of plasmid in a 20 μL reaction mixture which contained variable volumes of 1 and H8qasesc previously dissolved in DMSO to the stock concentration of 10 mM and 40 mM bicarbonate buffer (pH 8.4) at 37 °C, for 90 minutes. The reaction mixtures were vortexed from time to time. The reaction was terminated by short centrifugation RCF of $6708 \times g$ and addition of 5 μL of loading buffer (0.25% bromophenol blue, 0.25% xylene cyanol FF and 30% glycerol in TAE buffer, pH 8.24 (40 mM Tris-acetate, 1 mM EDTA)).

The samples were subjected to electrophoresis on 1% agarose gel (Amersham Pharmacia-Biotech, Inc) prepared in TAE buffer pH 8.24. The electrophoresis was performed at a constant voltage (80 V) until bromophenol blue had passed through 75% of the gel. A Submarine Mini-gel Electrophoresis Unit (Hoeffer HE 33) with an EPS 300 power supply was used. After electrophoresis, the gel was stained for 30 min by soaking it in an aqueous ethidium bromide solution (0.5 μg/mL). The stained gel was illuminated under a UV transilluminator Vilber-

Lourmat (France) at 312 nm and photographed with a Nikon Coolpix P340 Digital Camera through filter DEEP YELLOW 15 (TIFFEN, USA).

Molecular docking studies

Randomly chosen X-ray crystal structures of dodecamer d(CGCGAATTCGCG)₂, PDB ID: 3U2N [S8] and human serum albumin (HSA), PDB ID: 1BJ5 [S9], were obtained from the Protein Data Bank (<http://www.rcsb.org/pdb>). The active sites were identified according to positions of crystallized ligands in the PDB structures. Ligands were removed, as well as water and ions and structures were prepared for docking using Autodock Tools 1.5.6. [S10,S11]. Docking was carried in Autodock Vina 1.1.2. [S12]. Grid box size was set to 24 × 24 × 24 Å and exhaustiveness to 250. All calculations were carried on PARADOX computer cluster (Scientific Computing Laboratory of the Institute of Physics, Belgrade, Serbia). The ligand H8qasesc and **1** were prepared using X-ray determined coordinates, with Gasteiger charge correction done with Chimera program [S13], as no charges were assigned for selenium atoms.

REFERENCES

- [S1] N. Filipovic, N. Polovic, B. Raskovic, S. Misirlic-Dencic, M. Dulovic, M. Savic, M. Niksic, D. Mitic, K. Anelkovic and T. Todorovic, *Monatsh. Chem.*, 2014, **145**, 1089–1099.
- [S2] Agilent. (2010) CrysAlis PRO. Yarnton, Oxfordshire, UK: Agilent Technologies.
- [S3] R. H. Blessing, *Acta Crystallogr. A*, 1995, **51**, 33–38.
- [S4] G.M. Sheldrick, *Acta Crystallogr. A*, 2008, **64**, 112–122.
- [S5] R. L. Prior, X. L. Wu and K. Schaich, *J. Agric. Food Chem.*, 2005, **53**, 4290–4302.
- [S6] S. Léonce, V. Pérez, S. Lambel, D. Peyroulan, F. Tillequin, S. Michel, M. Koch, B. Pfeiffer, G. Atassi, J. A. Hickman and A. Pierre, *Mol Pharmacol.*, 2001, **60**, 1383–1391.
- [S7] J. Sambrook, E.F. Fritsch and T. Maniatis, *Molecular Cloning: a Laboratory Manual*, Cold Spring Harbor Laboratory Press, USA, 2nd edn., 1989, pp. 133–134.
- [S8] D.G. Wei, W.D. Wilson and S. Neidle, *J. Am. Chem. Soc.*, 2013, **135**, 1369–1377.

- [S9] S. Curry, H. Mandelkow, P. Brick and N. Franks, *Nat. Struct. Biol.*, 1998, **5**, 827–835.
- [S10] M. F. Sanner, *J. Mol. Graphics Modell.*, 1999, **17**, 57–61.
- [S11] G.M. Morris, R. Huey, W. Lindstrom, M.F. Sanner, R.K. Belew, D.S. Goodsell and A.J. Olson, *J. Comput. Chem.*, 2009, **16**, 2785–2791.
- [S12] O. Trott and A.J. Olson, *J. Comput. Chem.*, 2010, **31**, 455–461.
- [S13] E.F. Pettersen, T.D. Goddard, C.C. Huang, G.S. Couch, D.M. Greenblatt, E.C. Meng and T.E. Ferrin, *J. Comput. Chem.*, 2004, **25**, 1605–1612.